

Beam Time Request for SoLID

J. P. Chen, E. Chudakov, A. Deur, O. Hansen, C. W. de Jager, D. Gaskell,
J. Gomez, D. Higinbotham, J. LeRose, R. Michaels, S. Nanda, A. Saha,
P. Solvignon, V. Sulkosky, and B. Wojtsekhowski
Jefferson Lab, Newport News, VA 23606

P. A. Souder (*Contact **) L. Zana, and R. Holmes
Syracuse University, Syracuse, NY 13244

S. Johnston, K. Kumar, J. Mammei, L. Mercado, R. Miskimen, S. Riordan, and J. Wexler
University of Massachusetts Amherst, Amherst, MA 01003

H. Baghdasaryan, G. D. Cates, D. Crabb, M. Dalton, D. Day, N. Kalantarians, N. Liyanage,
V. V. Nelyubin, B. Norum, K. Paschke, O. A. Rondon, M. Shabestari,
J. Singh, A. Tobias, K. Wang, and X. Zheng
University of Virginia, Charlottesville, VA 22904

J. Arrington, K. Hafidi, P. E. Reimer, and J. Singh.
Argonne National Laboratory, Argonne, IL 60439

D. Armstrong, and T. Averett
College of William and Mary, Williamsburg, VA 23173

P. Decowski
Smith College, Northampton, MA 01063

L. El Fassi, R. Gilman, R. Ransome, and E. Schulte
Rutgers, The State University of New Jersey, Piscataway, NJ 08855

W. Chen, H. Gao, M. Huang, G. Laskaris, X. Qian, Y. Qiang, Q.J. Ye, and Q. Ye
Duke University, Durham, NC 27708

K. A. Aniol
California State University, Los Angeles, CA 90032

F. Meddi and G. M. Urciuoli
Dipartimento di Fisica dell'Università La Sapienza INFN, Sezione di Roma, I-00185 Roma, Italy

A. Lukhanin, Z. E. Meziani, and B. Sawatzky
Temple University, Philadelphia, PA 19122

P. M. King and J. Roche
Ohio University, Athens, OH 45701

E. Beise
University of Maryland, College Park, MD 20742

W. Bertozzi, S. Gilad, W. Deconinck, S. Kowalski, and B. Moffit
Massachusetts Institute of Technology, Cambridge, MA 02139

F. Benmokhtar, G. Franklin, B. Quinn
Carnegie Mellon University, Pittsburgh, PA 15213

G. Ron
Tel Aviv University, Tel Aviv, Israel 69978

T. Holmstrom
Longwood University, Farmville, VA 23909

P. Markowitz
Florida International University, Miami, FL 33199

X. Jiang
Los Alamos National Laboratory, Los Alamos, NM 87544

W. Korsch
University of Kentucky, Lexington, KY 40506

J. Erler
Universidad Autónoma de México, 01000 México D. F., México

M. J. Ramsey-Musolf
University of Wisconsin, Madison, WI 53706

C. Keppel
Hampton University, Hampton, VA 23668

H. Lu, X. Yan, Y. Ye, and P. Zhu
University of Science and Technology of China, Hafei, 230026, P. R. China

N. Morgan and M. Pitt
Virginia Tech, Blacksburg, VA 24061

J.-C. Peng
University of Illinois, Urbana-Champaign, IL 61820

H. P. Cheng, R. C. Liu, H. J. Lu, and Y. Shi
Institute of Applied Physics, Huangshan University, Huangshan, P. R. China

S. Choi, Ho. Kang, Hy. Kang, B. Lee, and Y. Oh
Seoul National University, Seoul 151-747, Korea

J. Dunne and D. Dutta
Mississippi State University, Mississippi State, MS 39762

K. Grimm, K. Johnston, N. Simicevic, and S. Wells
Louisiana Tech University, Ruston, LA 71272

O. Glamazdin and R. Pomatsalyuk
NSC Kharkov Institute for Physics and Technology, Kharkov 61108, Ukraine

Z. G. Xiao
Tsinghua University, Beijing, P. R. China

B.-Q. Ma and Y. J. Mao
School of Physics, Beijing University, Beijing, P. R. China

X. M. Li, J. Luan, and S. Zhou
China Institute of Atomic Energy, Beijing, P. R. China

B. T. Hu, Y. W. Zhang, and Y. Zhang
Lanzhou University, Lanzhou, P. R. China

C. M. Camacho, E. Fuchey, C. Hyde and F. Itard
LPC Clermont, Université Blaise Pascal CNRS/IN2P3 F-63177 Aubière, France

A. Deshpande
SUNY Stony Brook, Stony Brook, NY 11794

A. T. Katramatou and G. G. Petratos
Kent State University, Kent, OH 44242

J. W. Martin
University of Winnipeg, Winnipeg, MB R3B 2E9, Canada

E. Cisbani, S. Frullani and F. Garibaldi
INFN, Gruppo Collegato Sanità and Istituto Superiore di Sanità, I-00161 Rome, Italy

M. Capogni
*Istituto Nazionale di Metrologia delle Radiazioni Ionizzanti ENEA,
and INFN - Gruppo Collegato Sanità, I-00161 Rome, Italy*

V. Bellini, A. Giusa, F. Mammoliti, G. Russo and M.L. Sperduto
*INFN Sezione di Catania and Dipartimento di Fisica e Astronomia,
Università di Catania, I-95123 Catania, Italy*

C.M. Sutura
INFN Sezione di Catania and Università di Catania, I-95123 Catania, Italy

December 1, 2010

* e-mail: souder@physics.syr.edu

1 Introduction

This document is a brief update to the proposals PR-10-007 and E09-012. The experiment was approved by the PAC 35. Quoting the PAC 35 report, “the PAC believes the mission of this and future experiments using SoLID are sufficiently important that the Laboratory should make every effort to assist in securing the necessary funding.” In this report, the physics motivation is outlined, and progress in the areas of simulations, GEM detectors, and radiative corrections are given. Finally, the beam time request is given.

We reiterate here the physics topics that become accessible with the advent of a longitudinally polarized 11 GeV electron beam via measurements of the parity-violating asymmetry A_{PV} in deep inelastic scattering (DIS) in the kinematic region of large Bjorken $x = Q^2/2M\nu$. A_{PV} is defined to be:

$$A_{PV} = \frac{\sigma_R - \sigma_L}{\sigma_R + \sigma_L} \quad (1)$$

where $\sigma_R(\sigma_L)$ is the cross-section for incident right-(left-) handed electrons. With the proposed data set over a broad kinematic range that can be obtained simultaneously, we are able to:

1. Search for new interactions beyond the Standard Model (SM) in a unique way. The special feature of PVDIS is that it is sensitive to axial-hadronic currents, yet is insensitive to unknown radiative corrections that cloud the interpretation of lower energy experiments sensitive to these currents.
2. Search for Charge Symmetry violation (CSV) at the quark level.
3. Search for higher-twist effects in the parity-violating asymmetry. Significant higher-twist effects are observed in DIS cross sections, but in PVDIS large higher-twist contributions can only be due to quark-quark correlations.
4. Measure the d/u ratio in the proton, without requiring any nuclear corrections.
5. Determine if additional CSV is induced in heavier nuclei. Such an effect would have profound implications for our understanding of the EMC effect.

The unique opportunities for experiments on parity-violation at Jlab with the 11 GeV upgrade were recognized in the NSAC long-range planning exercises and elaborated on in the original proposal.

2 Review of the Motivation

The general expression for A_{PV} is[1]

$$A^{PV} = - \left(\frac{G_F Q^2}{4\sqrt{2}\pi\alpha} \right) \left[g_A^e Y_1 \frac{F_1^{\gamma Z}}{F_1^\gamma} + \frac{g_V^e}{2} Y_3 \frac{F_3^{\gamma Z}}{F_1^\gamma} \right] = - \left(\frac{G_F Q^2}{4\sqrt{2}\pi\alpha} \right) (Y_1 a_1 + Y_3 a_3). \quad (2)$$

The Y_i are functions of the kinematic variable $y = \nu/E$ and the ratios of structure functions $R^j(x, Q^2)$:

$$Y_1(x, y, Q^2) = \frac{1 + (1-y)^2 - y^2(1-r^2/(1+R^{\gamma Z})) - 2xyM/E}{1 + (1-y)^2 - y^2(1-r^2/(1+R^\gamma)) - 2xyM/E} \left(\frac{1 + R^{\gamma Z}}{1 + R^\gamma} \right) \quad (3)$$

$$Y_3(x, y, Q^2) = \frac{1 - (1-y)^2}{1 + (1-y)^2 - y^2(1-r^2/(1+R^\gamma)) - 2xyM/E} \left(\frac{r^2}{1 + R^\gamma} \right) \quad (4)$$

The above expressions are quite general.

In order to account for possible violations of the Standard Model, it is essential to express the parity-violating part of the electron-hadron interaction in terms of general phenomenological four-fermion contact interactions. couplings C_{ij}

$$\mathcal{L}^{PV} = \frac{G_F}{\sqrt{2}} [\bar{e}\gamma^\mu\gamma_5 e (C_{1u}\bar{u}\gamma_\mu u + C_{1d}\bar{d}\gamma_\mu d) + \bar{e}\gamma^\mu e (C_{2u}\bar{u}\gamma_\mu\gamma_5 u + C_{2d}\bar{d}\gamma_\mu\gamma_5 d)]$$

with additional terms as required for the heavy quarks. Here C_{1j} (C_{2j}) gives the vector (axial-vector) coupling to the j^{th} quark. For the Standard Model:

$$C_{1u} = g_A^e g_V^u \approx -\frac{1}{2} + \frac{4}{3} \sin^2 \theta_W \approx -0.19 \quad (5)$$

$$C_{1d} = g_A^e g_V^d \approx \frac{1}{2} - \frac{2}{3} \sin^2 \theta_W \approx 0.34 \quad (6)$$

$$C_{2u} = g_V^e g_A^u \approx -\frac{1}{2} + 2 \sin^2 \theta_W \approx -0.030 \quad (7)$$

$$C_{2d} = g_V^e g_A^d \approx \frac{1}{2} - 2 \sin^2 \theta_W \approx 0.025 \quad (8)$$

The numerical values include electroweak radiative corrections. The key point is that the C_{1i} are about an order of magnitude larger than the C_{2i} , which makes the a_1 term dominant.

As recently pointed out by Mantry, et al., [2] for the deuteron where $I = 0$, $Y_1 = 1$ and

$$a_1^D(x) = g_A^e \frac{F_1^{D\gamma Z}}{F_1^{D\gamma}} = a_1^D(x) = \frac{6}{5}(2C_{1u} - C_{1d}) \left(1 + \frac{2s^+}{u^+ + d^+}\right)$$

The only corrections to these formulae are physics beyond the Standard Model, CSV and quark-quark correlations, which form the motivation for the experiment, and known corrections including strange quarks and target mass corrections.

For the a_3 term, we use the quark-parton model (QPM), which describes the structure functions in terms of parton distribution functions (PDF's) functions $f_i(x)$ ($\bar{f}_i(x)$), which are the probabilities that the i^{th} quark (antiquark) carries a fraction x of the nucleon momentum. With the definitions $f_i^\pm = f_i \pm \bar{f}_i$, $y = \nu/E$, the structure functions are given by

$$F_1^\gamma = \frac{1}{2} \sum_i Q_i^2 (f_i(x) + \bar{f}_i(x))$$

$$F_1^{\gamma Z} = \sum_i Q_i g_V^i (f_i(x) + \bar{f}_i(x))$$

$$F_3^{\gamma Z} = 2 \sum_i Q_i g_A^i (f_i(x) - \bar{f}_i(x)).$$

Then

$$a_3^D(x) = \frac{g_V^e F_3^{\gamma Z}}{2 F_1^\gamma} = 2 \frac{\sum_i C_{2i} Q_i f_i^-(x)}{\sum_i Q_i^2 f_i^+(x)} = \frac{6}{5}(2C_{2u} - C_{2d}) \left(\frac{u^+ - d^-}{u^+ + d^+}\right) + \dots$$

Contributions due to higher twist to this term can be obtained from neutrino scattering. The contribution of R^γ to A_{PV} is given in the Y_3 factor.

The key is that since $(2C_{2u} - C_{2d})$ is small, there is less sensitivity to the hadronic physics, whereas $(u^+ - d^-)(u^+ + d^+) \sim 1$ so that we are sensitive to new physics contributions to the C_{2i} .

The main goal of the experiment is to place a narrow error band on the C_{2i} plot of Figure 2. As explained in the proposal, extra Z -bosons, and SUSY are examples of models that can cause contributions to the C_{2i} .

3 Charge Symmetry Violation

The NuTeV experiment published a discrepancy with the Standard Model with a significance of about three sigma. The result stirred a lot of controversy, resulting in a serious re-evaluation of the work. Additional corrections, including changes in the Cabibbo angle, strange sea, and improved radiative corrections, have recently been made, but have changed the result very little.

One possible explanation of the NuTeV result is charge symmetry violation (CSV) in the PDF's. As discussed in the proposal, various authors have presented the case that this is a reasonable explanation. In the PDG, these

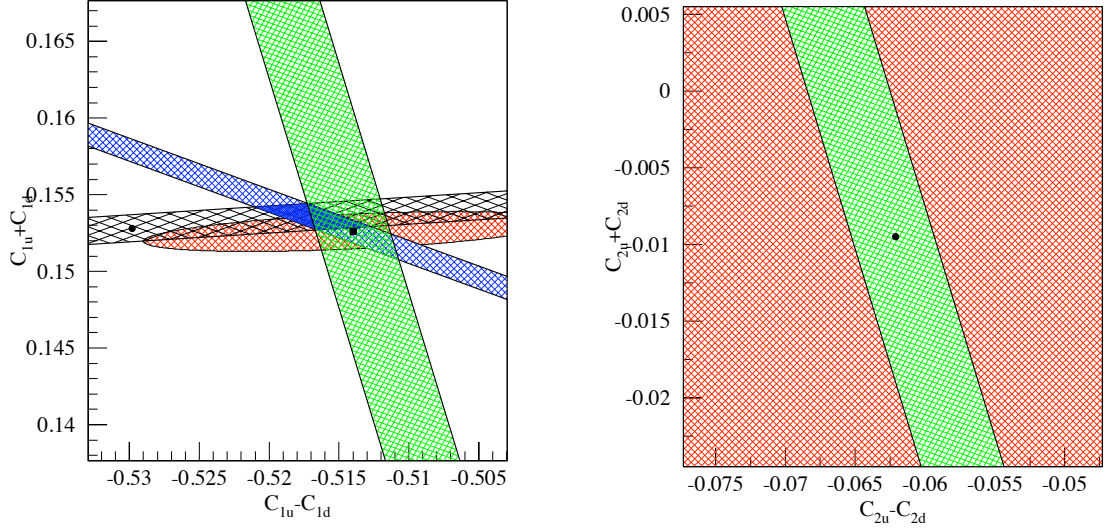


Figure 1: Green band: limits projected for this experiment. The blue band is the Qweak experiment and the black is the Cs APV.

CSV corrections have been applied; however, the NuTeV authors disagree with this procedure, citing the fact that CSV at this level have not been confirmed experimentally.

Our experiment is also sensitive to CSV. If the x -dependence of the CSV falls slower than the PDF's as suggested by the curves in Figure 2 our asymmetry should display a clear x -dependence. Moreover, these results will provide an important test of the CSV explanation for NuTeV. More details are given in our proposal.

3.1 Higher Twist

A recent paper has examined the contribution of higher twist (HT) effects to the dominant $Y_1 a_1$ term in A_{PV} . [2] The correction can be parameterized as a fractional contribution $R_1(HT)$ by

$$Y_1 a_1 \approx Y_1 a_1 (1 + R_1(HT) + \dots)$$

where the \dots refer to other corrections including CSV. It turns out that the only contribution comes from the operator

$$\mathcal{O}_{ud}^{\mu\nu} = \frac{1}{2} [\bar{u}(x) \gamma^\mu u(x) d(0) \gamma^\nu d(0) + (u \leftrightarrow d)]$$

which arises only from quark-quark correlations, or in other words, di-quarks in the nucleon. Higher twist contributions involving gluons cancel in the ratio. The special feature of A_{PV} is that it is the only practical experiment that can isolate higher twist due to four quarks.

The result is

$$R_1(HT) = -\frac{4}{5} \frac{(9 - 20 \sin^2 \theta_W) F_1^{\gamma;4q} - F_1^{\gamma Z;4q}}{(1 - \frac{20}{9} \sin^2 \theta_W) [u_p(x) + d_p(x)]}$$

where $F_1^{\gamma;4q}$ and $F_1^{\gamma Z;4q}$ are the four-quark higher twist contributions to the structure functions.

4 Data Sample and analysis

The observation of CSV is possible with our apparatus only if the effect varies with x . An x -independent CSV effect would be indistinguishable from a change in the C_{1q} 's. It is quite natural, however, to expect that the x -

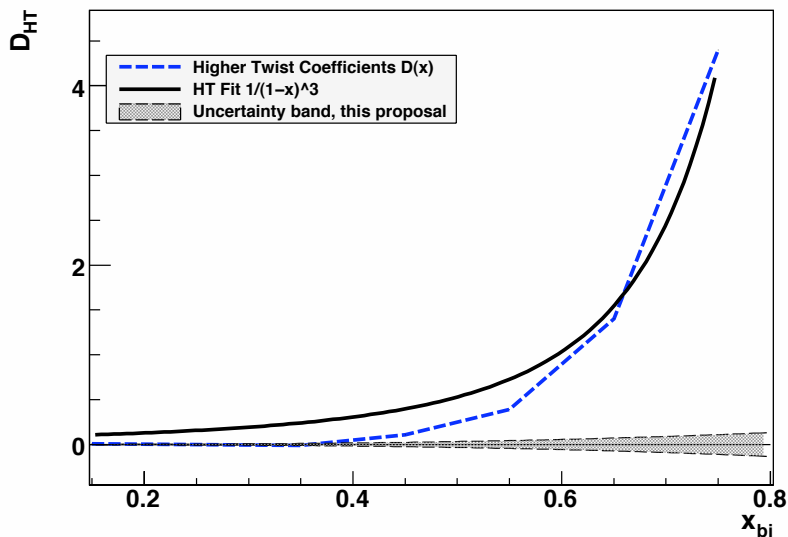


Figure 2: Possible contribution to A_{PV} due to CSV

dependence is similar to that shown in Figure 2, and we will make that assumption in our further discussion. From observations of higher-twist contributions to DIS cross sections, it is also natural to assume that Q^2 -dependent effects will also increase with increasing x .

To untangle the effects of hadronic and electroweak physics, we plan to fit the asymmetries to a function of the form

$$A_{PV}^D = A_{PV}^{EW} \left(1 + \beta_{HT} \frac{1}{(1-x)^3 Q^2} + \beta_{CSV} x^2 \right) \quad (9)$$

The resulting statistical errors on the fit parameters are:

$$\delta A_{PV}^{EW} / A_{PV}^{EW} = 0.3\%; \quad \delta \beta_{HT} = 0.0026; \quad \delta \beta_{CSV} = 0.017$$

With this method, we use the full statistical power of the data set. However, the result has some sensitivity to the exact form of the chosen fitting functions. Under the scenario where the hadronic effects are small, these errors are negligible as long as we assume that CSV and higher twist effects depend strongly on x , as expected. The one-sigma band for the CSV term is plotted in Figure 2.

If the pattern of higher twist effects is the same for A_{PV} as it is for the cross sections, then at $x = 0.6$ the asymmetries at the different Q^2 values will differ by 15%. In that scenario, the rapid x -dependence of the higher-twist coefficients for the cross section would imply that higher twist effects would still be negligible at $x = 0.4$. With a comparable x -dependence, a Q^2 -dependent effect as small as $\sim 1/30$ th of the effect seen in cross-section measurements would be easily identifiable given our statistical precision.

5 Plans for Simulations

Development of a full Geant4 simulation for the experiment in various configurations has begun. The goal of this work is to upgrade the existing simulation software to a modern version of Geant, fully evaluate configurations with several different magnets, provide code for optimization of the baffle design for such configurations, calculate background rates, and evaluate and optimize detector configurations and responses. We have two (three?) postdocs with experience in Geant4 simulations assigned to spending 30-40% of their time on this work in addition to the support of the collaboration.

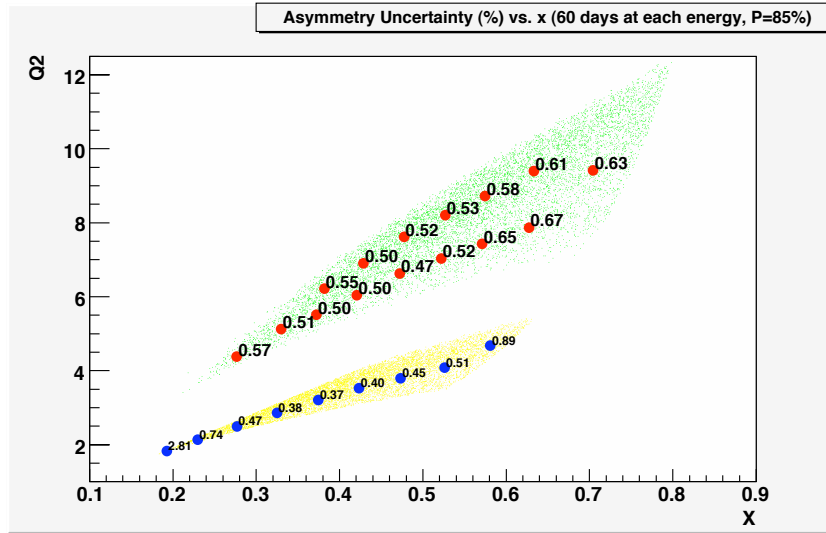


Figure 3: Anticipated statistical precision for Solid

Magnet design will be optimized using the software package Poisson Superfish, which can evaluate axially symmetric designs. Field configurations from this software can be exported and subsequently used in the Geant4 simulation. Our collaborators at ANL have agreed to provide significant contributions in this design process.

Detailed detector and tracking simulations are crucial in the design of the experiment. In particular, the GEM tracker configuration and PID must be demonstrated to be effective for our desired luminosities. Presently, a detailed GEM simulation and tracking code is being developed for the Hall A GEp-V experiment, E12-07-109, which also operates in an open, high luminosity environment. This simulation includes detailed geometry and material descriptions, individual GEM strip responses from electron drift, readout electronics, and full tracking using a tree search algorithm. One specific purpose for that work is to evaluate low energy backgrounds and the effect it has on tracking efficiencies and false tracks. Our collaboration overlaps with the GEp collaboration in some of these developments and we anticipate adapting this work to our simulation.

A set of milestones for the simulation development has been established. We anticipate having the aforementioned goals completed in approximately ten months with several groups working concurrently. This completion is expected to be before a foreseen technical review.

6 Progress with GEM's

The SoLID spectrometer requires high resolution track reconstruction under high rate conditions over a large area. A cost effective solution for large-area tracking in a high-rate environment is provided by the Gas Electron Multiplier (GEM) technology invented by F. Sauli [3] in 1997. The GEM is based on gas avalanche multiplication within small holes (on a scale of $100 \mu\text{m}$), etched in a Kapton foil with a thin layer of copper on both sides. The avalanche is confined in the hole resulting in very fast (about 10 ns rise time) signals. Several GEM foils (amplification stages) can be cascaded to achieve high gain and stability in operation. The relatively small transparency of GEM foils reduces the occurrence of secondary avalanches in cascaded GEM chambers. All these properties result in very high rate capabilities of up to 100 MHz per cm^2 and an excellent position resolution of $70 \mu\text{m}$. Fig. 5 illustrates the principle of operation of a triple (three foil) GEM chamber. Triple GEM chambers were successfully used in the COMPASS experiment at CERN [4]. One challenge we are facing for the GEM trackers of SoLID is the large active area required. The back trackers of SoLID need to have circular disk-type GEM chambers extending radially from 1 m to 2.25 m. These areas are significantly large compared to the

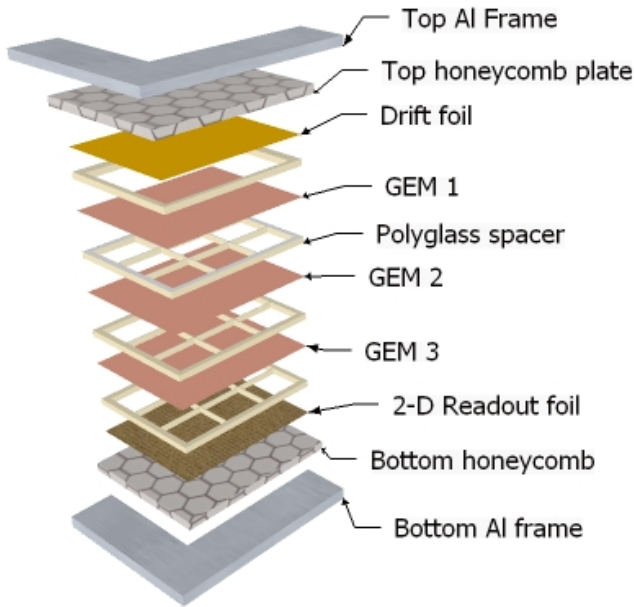


Figure 4: Schematic assembly view of one GEM chamber unit.

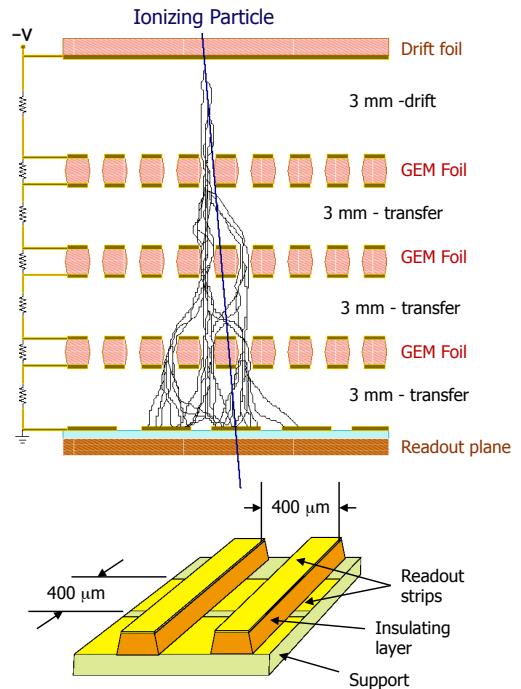


Figure 5: Top: Principle of triple GEM operation; bottom: 3D view of the readout board.

$32 \times 32 \text{ cm}^2$ area of the COMPASS chambers. In the past the maximum GEM foil area had been limited to $45 \times 50 \text{ cm}^2$. However, over the last few years the Micro Pattern Gas Detector (MPGD) group at CERN, in collaboration with INFN, has perfected two techniques to produce large area GEM foils: single mask GEM etching and GEM splicing [5, 6]. The single mask technique allows for the fabrication of foils as large as $60 \times 100 \text{ cm}^2$. The splicing technique allows for two such foils to be combined with only a 3 mm wide dead zone between the two foils (See Fig 5, right). The MPGD group has already succeeded in producing GEM foils as long as 95 cm and as wide as 66 cm. They are confident that they can fabricate GEM foils as large as $100 \times 200 \text{ cm}^2$ within two years using the two new techniques.

This new GEM technology is developed and shared through the CERN RD-51 collaboration (Collaboration for the development of micro-Pattern gas detectors technologies). Two of the groups responsible for GEM chambers of SoLID, INFN (Cisbani group) and UVa (Liyang group), are members of the RD-51 collaboration. These two groups are also leading an aggressive R&D program to develop large area GEM chambers for the hall A Super-Bigbite apparatus (SBS). The active area of large tracking chambers of SBS will be $50 \times 200 \text{ cm}^2$. These large GEM trackers will be assembled by combining five $40 \times 50 \text{ cm}^2$ “chamber modules” with narrow edges. The readout of the SBS and SoLID GEM chambers will be based on the APV25-S1 chip [7], currently in use for the COMPASS GEM trackers and the CMS silicon strip detectors.

The UVa and INFN groups successfully constructed and instrumented a prototype tracking telescope consisting of five $10 \text{ cm} \times 10 \text{ cm}$ GEM chambers. This tracker was installed on hall A left high resolution spectrometer for the PREX experiment. The GEM chambers worked well under very high rate conditions during the experiment yielding a track resolution of $\sim 70 \mu\text{m}$ (Fig 4). The INFN group is currently constructing a $40 \times 50 \text{ cm}^2$ prototype GEM chamber and an APV25-S1 based readout system. We plan to construct a second such prototype and a readout system at UVa in early 2011. We are planning a test run with the $10 \text{ cm} \times 10 \text{ cm}$ tracker plus the two $40 \times 50 \text{ cm}^2$ GEM chambers in hall A during the g2p/gep experiment scheduled for the summer of 2011.

An important issue concerning large GEM chambers is the high capacitance in long readout stripes. SoLID

requires readout stripes longer than 1 m and stripes longer than 0.5 m have not been used before. We will use the prototype chamber, with multiple readout stripes connected together, to study the impact of high stripe capacitance on resolution and noise.

Furthermore, there are several other large area GEM detector projects currently underway around the world [8, 9].

Given this rapid progress towards large area GEM chambers, we do not anticipate any serious technical difficulties facing the fabrication of SoLID GEM trackers.



Figure 6: GEM chambers of the prototype tracker being prepared for the beam tests during hall A PREX experiment.

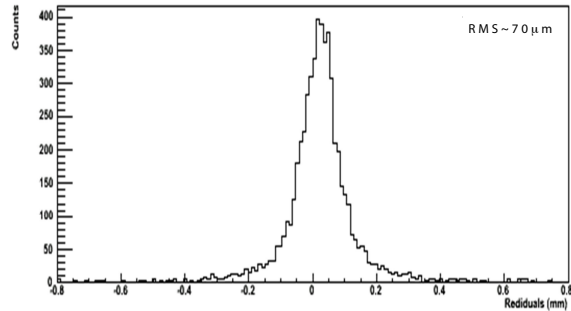


Figure 7: The residual distribution for one GEM projection, showing the high resolution achieved from our prototype GEM chambers.

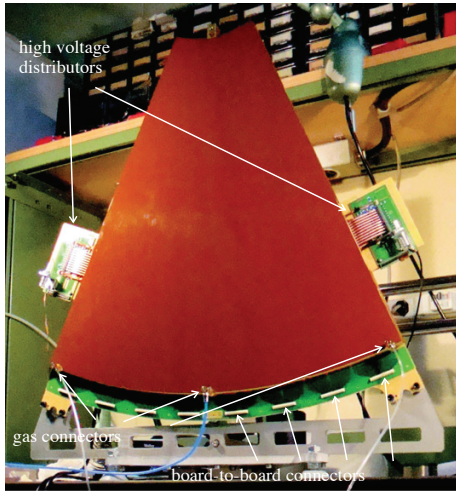
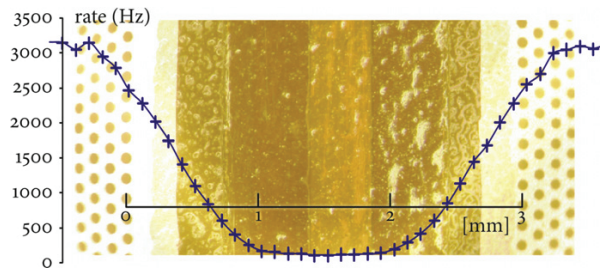
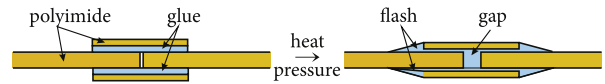


Figure 8: Left: Large area GEM prototype built at CERN for a possible future upgrade of the TOTEM detector. For this chamber 33 cm × 66 cm GEM foils were spliced together to make 66 cm × 66 cm foils. Right top: The principle of GEM splicing. Right bottom: Microscope image of the seam and the results of a X-ray scan showing the ~ 3 mm dead-area. (Figures from Rui De Oliveira, 5th RD51 Collaboration Meeting, Friburg, Germany, May 2010)



7 Radiative Corrections

We have started estimating the sensitivity of the experiment to radiative corrections. One important contribution is elastic scattering. The elastic events due to initial state radiation have significantly smaller Q^2 , resulting in a dilution of the asymmetry. Hence we would like the fraction of elastic events to be below 10%. In Figures 7, we see that this criteria is satisfied for both 6.6 and 11 GeV data.

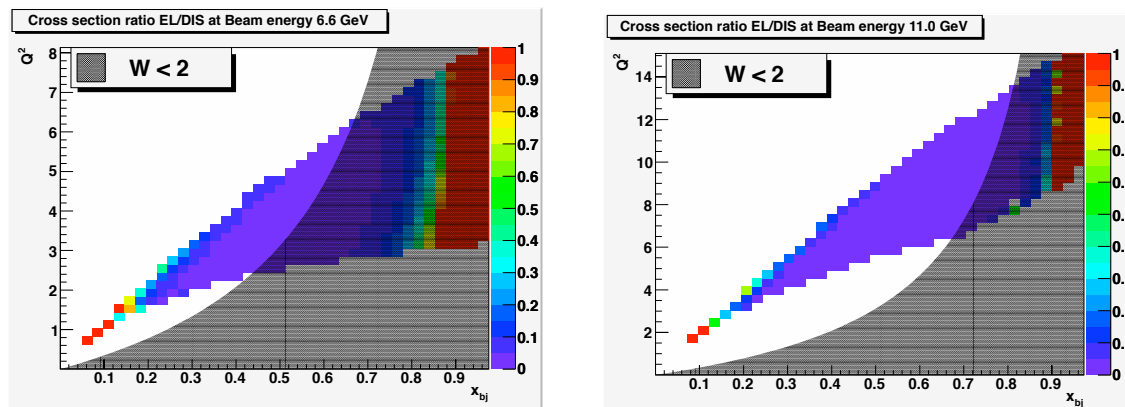


Figure 9: Ratio of elastic tail to DIS data for 6.6 GeV (left) and 11 GeV (right).

8 Beam Time Request

For the deuterium data, we have based our sensitivity on 180 days of production running at $50 \mu\text{A}$, with 1/3 of the data at 6.6 GeV and the rest at 11 GeV. Approximately 27 additional days, run at various currents, will be required for checkout and calibrations. An additional 18 days will be required at 4.4 GeV and $50 \mu\text{A}$ for radiative correction measurements. The total beam request at all energies for the deuterium measurement is 225 days, with about 25 of those days run mostly at reduced beam currents.

For the hydrogen measurement, 90 days are needed for production data at 11 GeV, about 9 days are required at 4.4 GeV to control radiative corrections and another 14 days will be required for calibration. The running time requested for hydrogen totals to 113 days.

In the future, we would also anticipate requesting an additional comparable run for a heavy nucleus such as Pb.

References

- [1] T. Hobbs and W. Melnitchouk, Phys. Rev. D **77**, 114023 (2008) [arXiv:0801.4791 [hep-ph]].
- [2] S. Mantry, M. J. Ramsey-Musolf and G. F. Sacco, arXiv:1004.3307 [hep-ph].
- [3] F. Sauli, Nucl. Inst. and Meth. **A386**, 531 (1997).
- [4] B. Ketzer *et al.*, Nucl. Phys. B (Proc. Suppl.) **125**, 368 (2003).
- [5] M. Villa, *etal.*, Nucl. Inst. and Meth. **A** (2010), doi:10.1016/j.nima.2010.06.312.
- [6] M. alfonsi *et al.*, Nucl. Inst. and Meth. **A617**, 151 (2010).
- [7] M.J. French *et al.*, Nucl. Instr. and Meth. **A 466** (2001) 359-365.

- [8] F. Simon *et al.*, “The Forward GEM Tracker of STAR at RHIC”, arXiv:0811.2432v1 [physics.ins-det].
- [9] S. D. Pinto, “Large GEMs for TOTEM T1 upgrade”, <http://indico.cern.ch/getFile.py/access?contribId=16&sessionId=2&resId=0&materialId=slides&confId=25069>